

STATUS OF THE RFX EXPERIMENT

V. ANTONI, L. APOLLONI, M. BAGATIN, W. BAKER, R. BARTIROMO, M. BASSAN, F. BELLINA, P. BETTINI, R. BILATO, T. BOLZONELLA, A. BUFFA, P. CAMPOSTRINI, S. CAPPELLO, L. CARRARO, E. CASAROTTO, R. CAVAZZANA, F. CHINO, G. CHITARIN, S. COSTA, A. DE LORENZI, D. DESIDERI, P. FIORENTIN, E. GAIO, L. GARZOTTI, L. GIUDICOTTI, F. GNESOTTO, M. GUARNIERI, S. GUO, O. HEMMING, P. INNOCENTE, A. LUCHETTA, G. MALESANI, G. MANDUCHI, G. MARCHIORI, L. MARRELLI, P. MARTIN, E. MARTINES, S. MARTINI, A. MASCHIO, A. MASIELLO, M. MORESCO, A. MURARI, P. O'LEARY, R. PACCAGNELLA, R. PASQUALOTTO, S. PERUZZO, R. PIOVAN, N. POMARO, R. PUGNO, M.E. PUIATTI, G. ROSTAGNI, A. SARDELLA, F. SATTIN, P. SCARIN, G. SERIANNI, P. SONATO, E. SPADA, A. STELLA, C. TALIERCIO, V. TOIGO, L. TRAMONTIN, F. TREVISAN, M. VALISA, S. VITTURI, Y. YAGI, P. ZACCARIA, E. ZILLI, G. ZOLLINO

Group for Fusion Research,
Euratom-ENEA-CNR-Universita di Padova Association,
Padua, Italy

Abstract

STATUS OF THE RFX EXPERIMENT.

The first results obtained in the RFX reversed field pinch experiment after the 1995 machine modifications are reported. The confinement, for fully stationary discharges at 0.6 MA, has now reached the expected values, even in the presence of MHD wall locked modes. Studies on locked mode effects have evidenced currents flowing from the plasma into the vessel in the region of locking. Measurements on plasma rotation and radial electric field have shown a perpendicular velocity shear at the edge similar to what is found in tokamaks and stellarators. New measurements on edge superthermal electrons and some evidence of their correlation with plasma core characteristics are included.

1. INTRODUCTION

The RFX reversed field pinch (major and minor radii 2.0 and 0.46m, respectively; maximum design current 2 MA) [1] began experiments in 1992 [2]. With one short break, it operated successfully up to 1995, establishing a detailed database at a plasma current of about 500 kA, with different set-up modes and a certain range of densities [3]. The plasma parameters were broadly in agreement with the expectations, and the maximum obtained value of the energy confinement time, τ_E - 1.5 ms, agreed with RFP scaling [4]. Some studies at were carried out 0.8 MA.

The loop voltage contained an anomalous (non-Spitzer) component [5] attributed in part to field errors, as is often the case; locked modes were always observed and proved difficult to control [6]. In 1995, RFX was shut down for machine improvements, including field error reduction by closing the outer equatorial gap and partially closing one poloidal gap, installation

of an eight pellet injector, and a new boronization system with diborane, in order to fit new diagnostics.

This paper describes the obtained plasma improvements, including increased τ_E and β , a 10% reduction in the loop voltage accompanied by much better pulse reproducibility and insensitivity to small residual field errors. We also present new results on locked modes, plasma-vessel currents, particle confinement using pellet injection, plasma rotation (globally from spectroscopy and close to the edge by Langmuir probes) and new edge measurements of superthermal electrons.

2. EFFECT OF MACHINE MODIFICATIONS ON PLASMA PERFORMANCE

As a consequence of the equatorial gap short-circuit, the fluctuating radial field at the gap has been reduced by a factor of two to three; during flat-top it remains below 1 % of the main poloidal field $B_\theta(a)$. The closure of one poloidal gap, together with an improvement of the equilibrium feedback control system, reduced the maximum radial field through the vertical gaps to less than 4% of the main poloidal field and to ~ 1 % in the optimized pulses [7]. The effect of shell gap closure resulted, at 0.6 MA, in better pulse reproducibility, with reduced scatter of data and a more reliable density behaviour under the same experimental conditions. A global decrease of $\sim 10\%$ (Fig. 1) in loop voltage and a corresponding increase in the energy confinement time were obtained. β_θ remained essentially unchanged. The voltage reduction corresponds to a decrease in the anomalous voltage from -15 to -12 V [8].

Gap field errors and shift are now kept within a range where their influence on the loop voltage is negligible [7]. The remaining portion of anomalous voltage can probably be attributed to the magnetic field distortion due to the MHD locked modes.

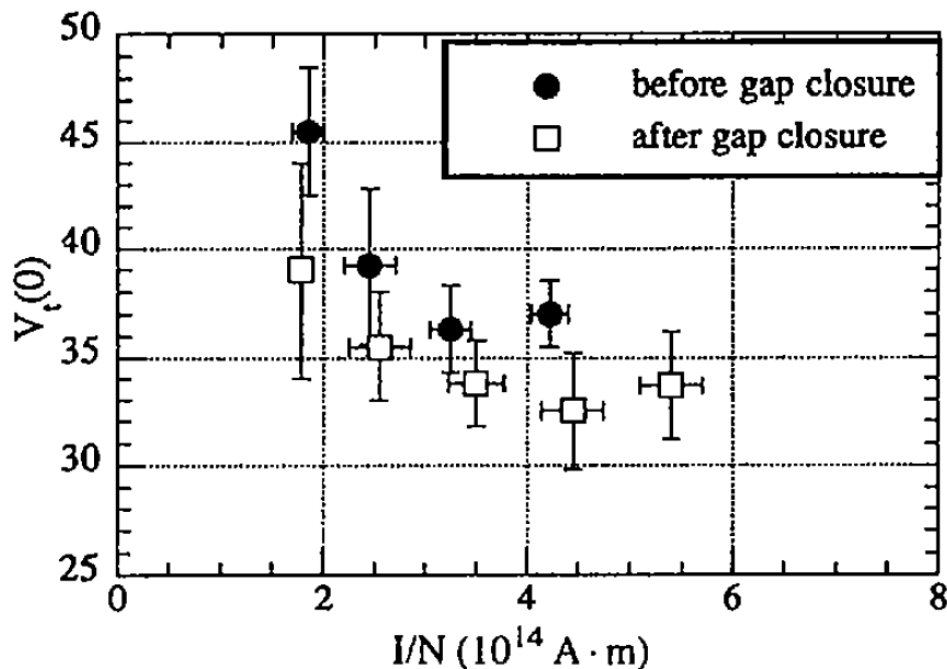


FIG. 1. Loop voltage during the current flat-top versus I/N , the ratio between the toroidal plasma current, I , and the average line density, N .

3. GLOBAL PERFORMANCE AT 0.6 MA

After a graphite boronization by diborane (which allowed the achievement of $Z_{\text{eff}} \sim 1.2$), an extensive exploration of the dependence of plasma performance on the density for fully sustained discharges at 0.6 MA has been carried out. As shown in Fig. 2, both β_θ and τ_E increase monotonically as the density is raised up to the maximum value compatible with sustained discharges in the present conditions of operation, obtained at $I/N > 1 \times 10^{-14}$ A·m.

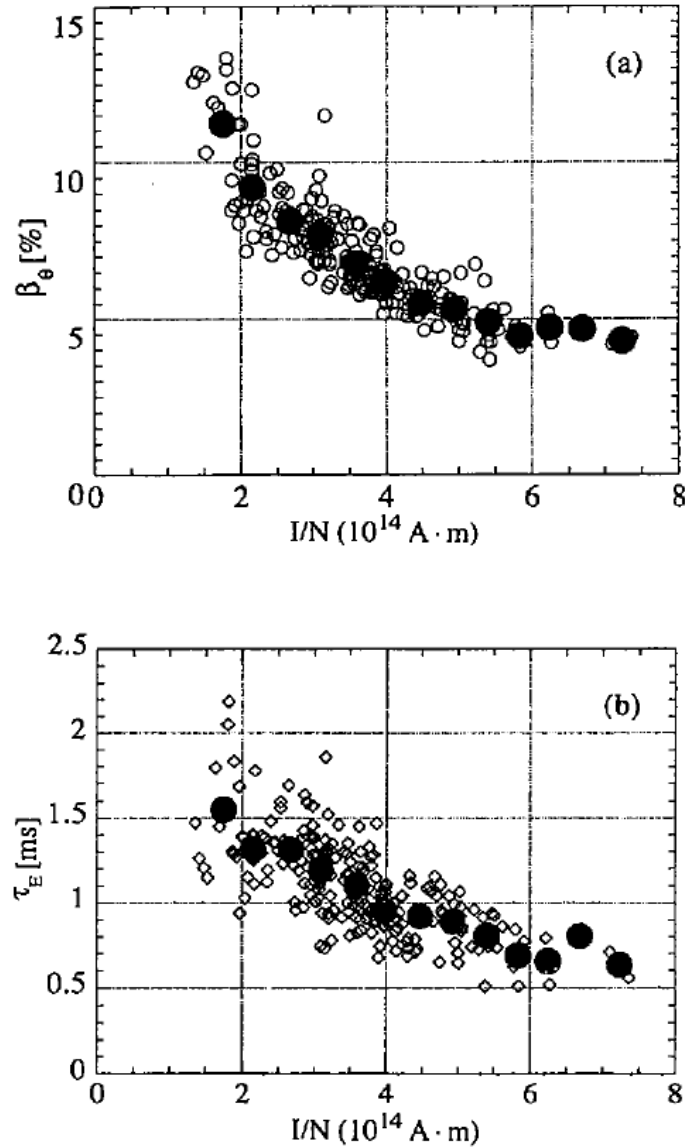


FIG. 2. (a) Poloidal β ($\beta_e = 2 \beta_{\theta e}$) and (b) energy confinement time versus I/N . Solid circles: ensemble averages of data.

The average β_θ reaches $\sim 11\%$ and $\tau_E \sim 1.5$ ms, with maximum τ_E values exceeding 2 ms. The total radiated power, measured by absolutely calibrated bolometric tomography (Fig. 3), is normally between 5 and 10% of the input power for I/N above 3×10^{-14} A·m. At lower I/N the radiation increases, reaching 20% of the input power at the minimum I/N value ($> 1 \times 10^{-14}$ A·m), where it has been possible to sustain a stationary discharge. At I/N lower than 1×10^{-14} A·m, the

loop voltage is so high that no steady state can be obtained and the plasma current decays. In any case, even in these conditions, there is no evidence of plasma disruptions. The radiation emission is always concentrated at $r/a > 0.75$.

4. LOCKED MODES AND PLASMA CURRENT FLOWING INTO THE VESSEL

Despite the improvements in the overall confinement, in RFX an anomalous loss effect remains, related to stationary magnetic disturbances still present in all pulses, because of MHD locked modes. These locked modes cause a local helical deformation of the magnetic surfaces extending for about 30-40° toroidally, driving large local dissipation of power and helicity.

Parallel power fluxes of the order of 100 MW/m^2 were measured in the 1994 campaigns [9], mostly caused by superthermal electrons flowing along the field lines, which heated the tiles up to 2000°C in the region where the graphite wall was intersected by the distorted magnetic surfaces. Tile heating led to an enhancement of the influx of carbon by a factor of ~ 100 , of oxygen by a factor of ~ 40 and of hydrogen by a factor of ~ 30 . In high current discharges (0.8-1 MA), the carbon tile temperature might reach values close to that of carbon sublimation (3350°C), resulting in frequent carbon blooming phenomena, with a consequent increase in Z_{eff} (from ~ 1.2 - 1.5 up to ~ 2) and in density, which caused a decrease in temperature and an increase in loop voltage [9]. Damages observed during the 1995 shutdown on the contact surface between the graphite tiles and the vacuum vessel have been ascribed to the effect of currents flowing poloidally from the plasma into the stiffening rings of the vacuum vessel. These currents have a dominant $m = 1$ mode; moreover, a strong toroidal asymmetry has been observed.

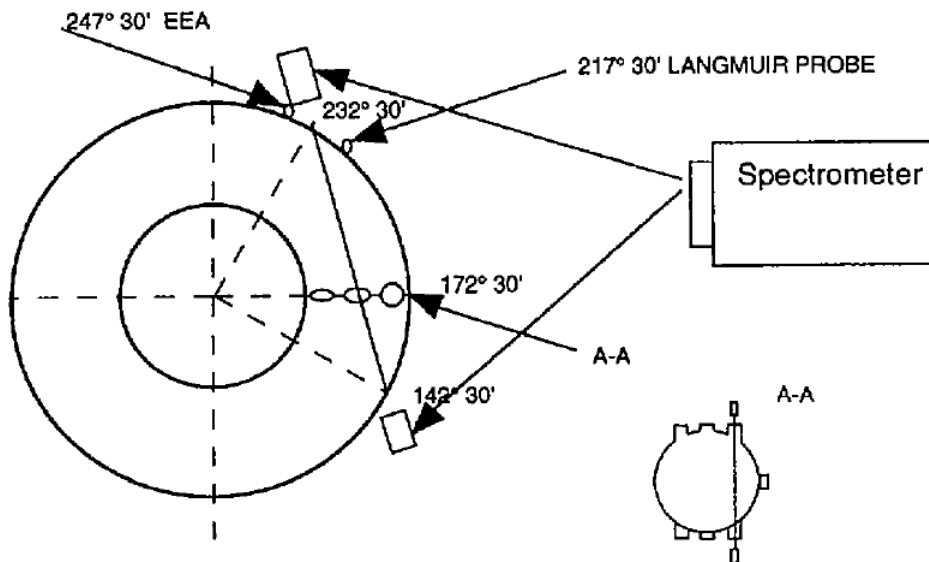


FIG. 4. Layout of spectroscopic and EEA diagnostics

Approximately 3 kA of current flowing through one graphite tile of the first wall and the vessel stiffening ring are necessary, on the basis of numerical and experimental evaluations, to obtain the damages observed in RFX [10]. On the assumption that the magnetic deformation has a toroidal extension of 30°, the total current flowing into the vessel for each shot was estimated to be of the order of 10% of the toroidal plasma current [9, 10].

A preliminary measurement of the poloidal voltage on the vacuum vessel has confirmed the presence of these currents in the region dominated by the helical perturbation with strong toroidal asymmetry. The measured voltage also shows a poloidal asymmetry and a resistive distribution of the current in the vessel. These currents are stationary during the shots, with the presence of a significantly high frequency oscillation. The maximum currents estimated from the voltage measurements amount to an average value between 1 and 2 kA for each vessel stiffening ring. This value is lower, by a factor of five to ten, than the value estimated on the basis of the observed damages. The difference can be ascribed to the strong toroidal asymmetry and the experimental operating conditions. Much work remains to be done to clarify these phenomena.

5. PLASMA ROTATION AND RADIAL ELECTRIC FIELD

Plasma flow and radial electric field have been measured both by spectroscopy and Langmuir probes (Fig. 4). The poloidal and toroidal rotation velocities of the impurities have been deduced from Doppler shift measurements on the lines of C V (2271 Å, fifth order), C III (2296 Å, fifth order), B IV (2823 Å, fourth order), O V (2781 Å, fourth order), C VI (5290 Å, second order). As shown in Table I, the toroidal velocity changes sign close to the toroidal field reversal surface ($r/a \sim 0.9$). The plasma flow measurements by Langmuir probes (Fig. 5) at the extreme edge detect the presence of parallel (nearly poloidal) and perpendicular (nearly toroidal) drifts with a velocity of $\sim 10^4$ m/s and a perpendicular velocity shear, $dv/dr \sim 10^6$ s⁻¹, comparable to what is found in tokamaks and stellarators.

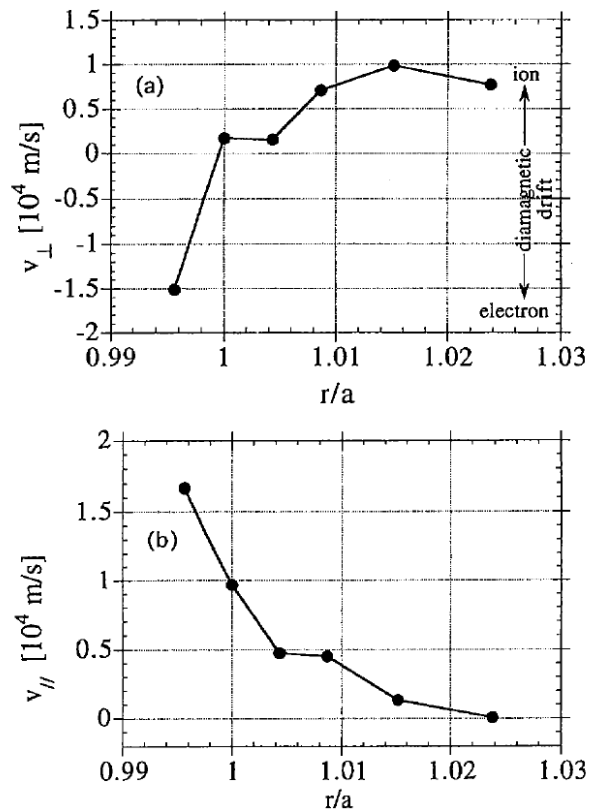


FIG. 5. Plasma flow velocity (a) perpendicular and (b) parallel to the magnetic field as functions of normalized radius.

TABLE I. TOROIDAL AND POLOIDAL ROTATION VELOCITIES OF IMPURITIES

| Ion | r/a | V_{tor} (10^3 m/s) | V_{pol} (10^3 m/s) |
|-------|-------|--------------------------------|--------------------------------|
| C III | 0.95 | (-5)-(-10) | 0-2 |
| O V | 0.9 | (-2)-1 | 1-4 |
| B IV | 0.8 | 2-4 | 0-5 |
| C V | 0.7 | 5-10 | 0-3 |
| C VI | 0.4 | 2-5 | — |

The perpendicular drift velocity of the impurities has the same direction of the majority ions. The plasma potential in the edge region measured by a fast insertion Langmuir probe (Fig. 6) shows that the radial electric field is directed inwards and changes sign when going deeper into the plasma, where it is in agreement with what is established in a stochastic magnetic field in order to restrain the electron flow.

The perpendicular drift is consistent with a drift velocity of $v_E = E_r/B_\theta$ due to the radial electric field. The perpendicular drift is in the ion diamagnetic drift direction at the extreme edge and changes sign when going deeper into the plasma. Langmuir probe measurements indicate that this change in sign is located between the first wall and the toroidal field reversal surface.

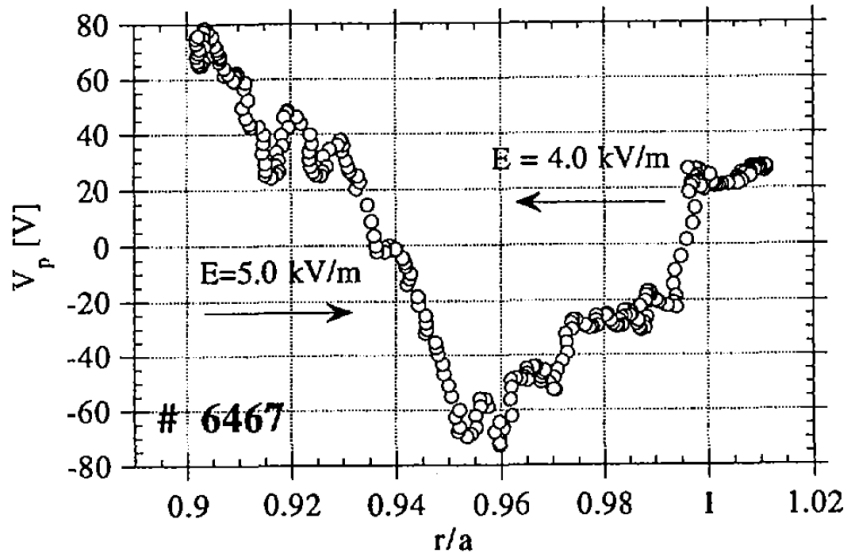


FIG. 6. Plasma potential as a function of normalized radius, showing inversion of the radial electric field.

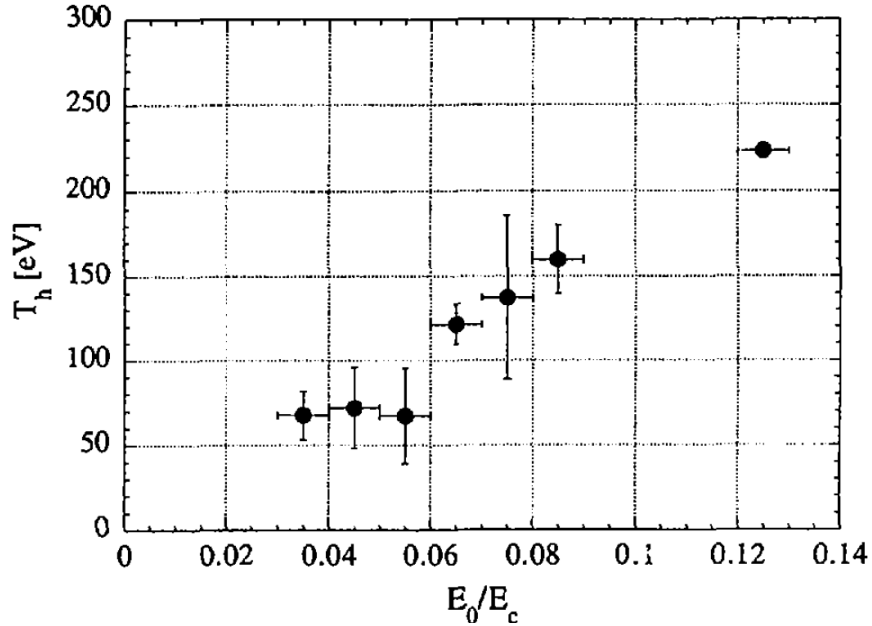


FIG. 7. Superthermal electron temperature as a function of the ratio between on-axis induced electric field and on-axis critical fields.

6. SUPERTHERMAL ELECTRONS AT THE EDGE

Superthermal electrons have been measured by an electrostatic electron energy analyser (EEA) developed at the Electrotechnical Laboratory of Tsukuba (Japan) and jointly operated in RFX [11]. A unidirectional flow of superthermal electrons along the magnetic field is observed with a backflow less than 10%. The energy distribution function is well approximated by a half-Maxwellian of temperature T_h . A relationship between T_h and the ratio between the on-axis applied electric field E_0 and the on-axis critical Dreicer field E_c is found (Fig. 7). This result suggests that superthermal electrons are produced at the centre of the plasma (as confirmed by pellet trajectories) and then are transported to the edge. Superthermal electrons are found to carry a large parallel current density at the edge, in the range of 200-600 kA/m².

To account for the maximum parallel energy flux at the edge (-100 MW/m²) measured by calorimeter probes and CCD cameras, equal parallel and perpendicular temperatures must be assumed.

7. PELLET INJECTION

A first programme of pellet experiments has been performed at currents of ≈ 0.6 MA: one or two pellets of small (1.5×10^{20} atoms) or intermediate (3×10^{20} atoms) size have been launched during the current flat-top phase with a speed of 500-900 m/s. The small pellets fired at low velocity (500-600 m/s) are completely ablated in the plasma, and large global density increases (typically, $\Delta n/n \approx 1$) are obtained, causing relatively small effects on plasma current and loop voltage.

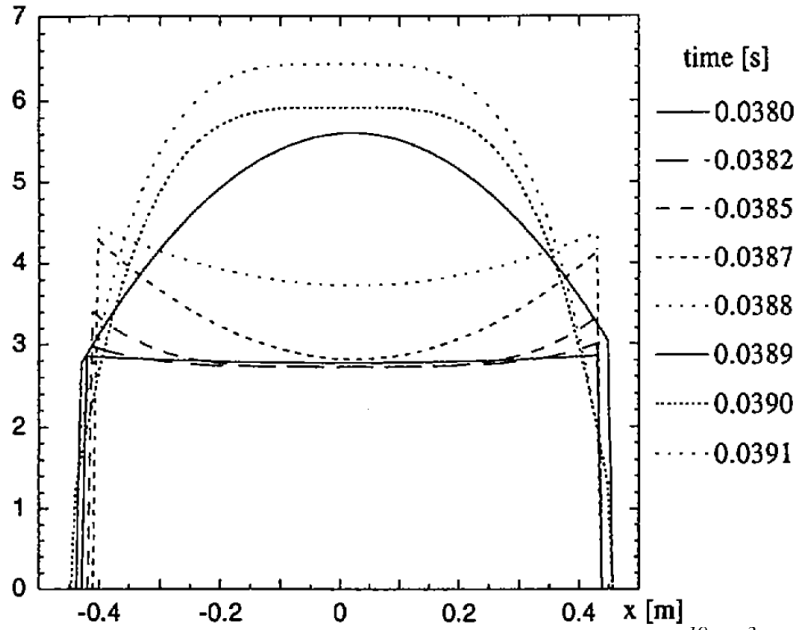


FIG. 8. Shot 6185 showing inverted n_e profiles (10^{19} m^{-3}).

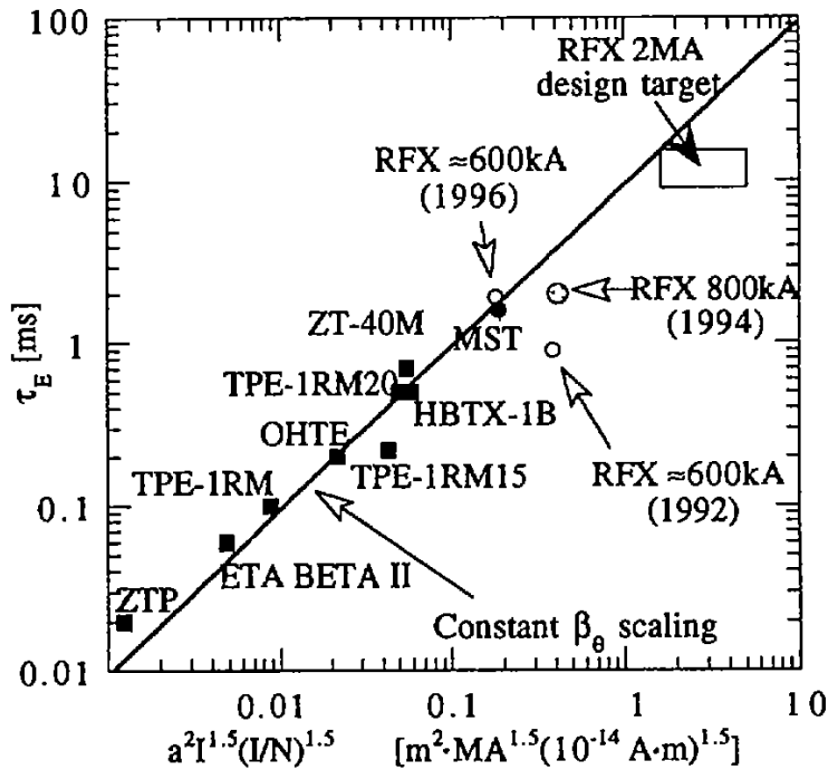


FIG. 9. Comparison of RFX data with optimum experimental confinement fit to Connor-Taylor scaling [13].

Even in the most perturbing cases, when $\Delta n/n = 2$ and the after-pellet plasma is in a high radiation regime, no disruptive process is excited. With optimized parameters, the pellets are

ablated in the plasma core, and the after-pellet density is well fitted by a parabolic profile on top of a constant pedestal (Fig. 8). A peaking factor of $n_c(0)/\langle n_c \rangle < 2$ is achieved, which decays in a few milliseconds.

The time behaviour of the density profiles indicates that the particle diffusion coefficient is $\approx 20\text{-}40 \text{ m}^2\cdot\text{s}^{-1}$ in the plasma core. Pellet trajectory deflections of 10^{-15} cm are measured, both toroidally and poloidally, which has been simulated by an NGPS ablation code [12] considering an asymmetric ablation by superthermal electrons flowing unidirectionally along field lines not only at the plasma edge but also in the plasma core. Estimates of τ_E after injection indicate a τ_E drop of 70-100 eV. The toroidal loop voltage increases by 2-3 V. Assuming that the T_c profile is unchanged, the value of β_θ and τ_E should be higher by 30-50% after injection, which is consistent with the empirical RFX scaling of β_θ with I/N (Fig. 2(a)).

8. CONCLUSIONS

After the recent machine modifications, which allowed a more accurate field error correction and a better control of plasma shift and shape, and by wall conditioning and boronization, which permitted operation at low Z_{eff} ($\sim 1.2\text{-}1.5$) and a better density control, RFX has, at 0.6 MA, achieved the expected performance (Fig. 9) in completely stationary discharges lasting up to 100 ms.

In order to achieve a similar control of the magnetic surfaces at higher currents, a more effective preionization system is required (in preparation).

The impact of locked modes on the discharge performance remains to be clarified. It has been observed that the helical deformation causes an increase in the impurity influx and the generation of currents flowing from the plasma to the first wall and the vessel. On the other hand, plasma rotation up to 10 km/s has been observed, even in the presence of locked modes.

Special attention has been paid to the study of edge physics, in order to clarify to which extent it may affect global confinement. Radial electric field and velocity shear comparable to those in tokamaks and stellarators have been identified.

Pellet experiments have permitted a first evaluation of the particle diffusion coefficient. Pellet trajectory deflection has proved the presence of superthermal electrons, also in the plasma core.

ACKNOWLEDGEMENTS

It is a pleasure to acknowledge Dr. H.A.B. Bodin's valuable suggestions. The authors wish to express their appreciation to the RFX technical staff.

REFERENCES

- [1] RFX TEAM, *Fus. Eng. Des.* (special issue) 25 4 (1995).
- [2] RFX TEAM, in *Plasma Physics and Controlled Nuclear Fusion Research 1992* (Proc. 14th Int. Conf. Würzburg, 1992), Vol. 2, IAEA, Vienna (1993) 583.
- [3] ANTONI, V., et al., in *Plasma Physics and Controlled Nuclear Fusion Research 1994* (Proc. 15th Int. Conf. Seville, 1994), Vol. 2, IAEA, Vienna (1994) 405.
- [4] BUFFA, A., GNESOTTO, F., in *Fusion Engineering* (Proc. 16th IEEE Symp. Urbana-Champaign 1995), Urbana-Champaign (1995) 1395.

- [5] CARRARO, L., et al, in Controlled Fusion and Plasma Physics (Proc. 22nd Eur. Conf. Bournemouth, 1995), Vol. 19C, Part III, European Physical Society, Geneva, (1995) 161.
- [6] BUFFA, A., et al., in Controlled Fusion and Plasma Physics (Proc. 21st Eur. Conf. Montpellier 1994), Vol. 18B, Part I, European Physical Society, Geneva (1994) 458.
- [7] BOLZONELLA, T, et al., in Controlled Fusion and Plasma Physics (Proc. 23rd Eur. Conf. Kiev, 1996), Vol. 20C, European Physical Society, Geneva (1996) c002.
- [8] BUFFA, A., RFX TEAM, *ibid.*, c001.
- [9] VALISA, M., et al., in Plasma-Surface Interactions (Proc. 12th PSI Conf. Saint-Raphael, 1996).
- [10] SONATO, P., et al., *ibid.*
- [11] YAGI, Y., et al., in Controlled Fusion and Plasma Physics (Proc. 23rd Eur. Conf. Kiev, 1996), Vol. 20C, European Physical Society, Geneva (1996)d001.
- [12] GARZOTTI, L., et al., *ibid.*, c003.
- [13] CONNOR, J.W., TAYLOR, J.B., *Phys. Fluids* 27 (1984) 2676.